


# Clinical features and diagnostic imaging of cholangiolocellular carcinoma compared with other primary liver cancers: a surgical perspective

Technology in Cancer Research & Treatment  
 Volume 19: 1-17  
 © The Author(s) 2020  
 Article reuse guidelines:  
[sagepub.com/journals-permissions](https://sagepub.com/journals-permissions)  
 DOI: 10.1177/1533033820948141  
[journals.sagepub.com/home/tct](https://journals.sagepub.com/home/tct)  


Hiroyuki Takamura, PhD, MD<sup>1,2</sup> , Ryosuke Gabata, MD<sup>2</sup>, Yoshinao Obatake, PhD, MD<sup>2</sup>, Shinichi Nakanuma, PhD, MD<sup>2</sup>, Hironori Hayashi, PhD, MD<sup>2</sup>, Kazuto Kozaka, PhD, MD<sup>3</sup>, Motoko Sasaki, PhD, MD<sup>4</sup>, Mitsuyoshi Okazaki, PhD, MD<sup>2</sup>, Takahisa Yamaguchi, PhD, MD<sup>2</sup>, Hiroyuki Shimbashi, PhD, MD<sup>2</sup>, Shiro Terai, PhD, MD<sup>2</sup>, Koichi Okamoto, PhD, MD<sup>2</sup>, Isamu Makino, PhD, MD<sup>2</sup>, Jun Kinoshita, PhD, MD<sup>2</sup>, Keishi Nakamura, PhD, MD<sup>2</sup>, Tomoharu Miyashita, PhD, MD<sup>2</sup>, Hidehiro Tajima, PhD, MD<sup>2</sup>, Itasu Ninomiya, PhD, MD<sup>2</sup>, Sachio Fushida, PhD, MD<sup>2</sup>, Azusa Kitao, PhD, MD<sup>3</sup>, Masaaki Kitahara, PhD, MD<sup>5</sup>, Kuniaki Arai, PhD, MD<sup>5</sup>, Taro Yamashita, PhD, MD<sup>5</sup>, Tatsuya Yamashita, PhD, MD<sup>5</sup>, Hiroko Ikeda, PhD, MD<sup>4</sup>, Yasunori Satoh, PhD, MD<sup>4</sup>, Kenichi Harada, PhD, MD<sup>4</sup>, Syuichi Kaneko, PhD, MD<sup>5</sup>, Toshihumi Gabata, PhD, MD<sup>3</sup>, Tateo Kosaka, PhD, MD<sup>1</sup>, and Tetsuo Ohta, PhD, MD<sup>2</sup>

## Abstract

**Background and Objectives:** Although cholangiolocellular carcinoma is considered a combined hepatocellular and cholangiocarcinoma, we feel that this classification is not appropriate. Therefore, we compared the diagnostic imaging findings, surgical prognosis, and pathological features of cholangiolocellular carcinoma with those of other combined hepatocellular and cholangiocarcinoma subtypes, hepatocellular carcinoma, and cholangiocarcinoma. **Methods:** The study patients included 7 with classical type combined hepatocellular and cholangiocarcinoma; 8 with stem cell feature, intermediate type combined hepatocellular and cholangiocarcinoma; 13 with cholangiolocellular carcinoma; 58 with cholangiocarcinoma; and 359 with hepatocellular carcinoma. All patients underwent hepatectomy or living-related donor liver transplantation from 2001 to 2014. **Results:** cholangiolocellular carcinoma could be distinguished from hepatocellular carcinoma, other combined hepatocellular and cholangiocarcinoma subtypes, and cholangiocarcinoma by the presence of intratumoral Glisson's pedicle, hepatic vein penetration, and tumor-staining pattern on angiography-assisted CT. Cholangiolocellular carcinoma was associated with a significantly lower SUV-max than that of cholangiocarcinoma on FDG-PET. Hepatocellular carcinoma, classical type, and cholangiolocellular carcinoma had significantly better prognoses than stem cell feature, intermediate type and cholangiocarcinoma. A cholangiocarcinoma component was detected in cholangiolocellular carcinoma that progressed to the hepatic hilum, and the cholangiocarcinoma component was found in perineural invasion and lymph node metastases. **Conclusions:** From the viewpoint of surgeon, cholangiolocellular carcinoma should be classified as a good-prognosis subtype of biliary tract carcinoma because of its

<sup>1</sup> General and Digestive Surgery, Kanazawa Medical University, Kahoku, Ishikawa, Japan

<sup>2</sup> Gastroenterologic Surgery, Kanazawa University, Kanazawa, Ishikawa, Japan

<sup>3</sup> Radiology, Kanazawa University, Kanazawa, Ishikawa, Japan

<sup>4</sup> Pathology, Kanazawa University, Kanazawa, Ishikawa, Japan

<sup>5</sup> Gastroenterology, Kanazawa University, Kanazawa, Ishikawa, Japan

## Corresponding Author:

Hiroyuki Takamura, General and Digestive Surgery, Kanazawa Medical University, 1-1 Daigaku, Uchinada, Kahoku-gun, Ishikawa 920-0293, Japan.  
 Email: [takamuh@kanazawa-med.ac.jp](mailto:takamuh@kanazawa-med.ac.jp)



tendency to differentiate into cholangiocarcinoma during its progression, and its distinctive imaging and few recurrence rates different from other combined hepatocellular and cholangiocarcinoma subtypes.

## Keywords

cholangiolocellular carcinoma, cholangiocarcinoma, bile ductular carcinoma, combined hepatocellular and cholangiocarcinoma

## Abbreviations

CC, cholangiocarcinoma; ChC, combined hepatocellular and cholangiocarcinoma; CK, cytokeratin; CLC, cholangiolocellular carcinoma; CT, computed tomography; CTAP, CT during arterial portography; CTHA, CT during hepatic arteriography; EVG, elastica van Gieson; FDG-PET, 18-fluoro-2-deoxyglucose positron-emission tomography; HCC, hepatocellular carcinoma; Hep-Par1, hepatocyte paraffin I; NCAM, neural cell adhesion molecule; SC-INT, intermediate cell subtype of combined hepatocellular and cholangiocarcinoma with stem cell features; SUV, standardized uptake value; WHO, World Health Organization

Received: April 23, 2019; Revised: June 21, 2020; Accepted: July 10, 2020.

## Introduction

Intrahepatic cholangiocarcinoma (CC) is generally classified as either large bile ductal central type or small bile ductal peripheral type; however, this classification may not be clinically appropriate, and biological characteristics such as histopathology should be taken into account when classifying CCs. Intrahepatic primary cancers with differentiation toward the biliary tract include combined hepatocellular and cholangiocarcinoma (ChC) and CC, but the pathological features are complicated and the 2010 World Health Organization (WHO) classification<sup>1</sup> (Table S1) may not be appropriate.

We therefore evaluated the characteristics of cancers with stem cell (SC) or CC components using diagnostic imaging, surgical results, and pathological features to determine an appropriate surgical strategy for primary liver cancers with bile duct components, such as ChC and CC. We previously defined peripheral CC that resembles the bile ductule as bile ductular carcinoma, which is also called cholangiolocellular carcinoma (CLC),<sup>2</sup> and investigated its various features, including molecular biological characteristics and imaging findings.<sup>3-9</sup> Although the 2010 WHO classification categorized CLC as a subtype of ChC with SC features, its definition is complicated. Hepatocellular carcinoma (HCC) components, SC-typical components, SC intermediate-cell (SC-INT) components, CLC components, and CC components have all been reported within tumors diagnosed as classical type ChC, SC-type ChC, or CC.<sup>3</sup> It is impossible to distinguish clearly between SC-typical and SC-INT subtypes as defined in the 2010 WHO classification because the pure SC-typical subtype is extremely rare and is classified together with the SC-INT subtype.<sup>10</sup>

CC has well-, moderately, and poorly differentiated biliary components, often accompanied by abundant stroma. Mucin may be demonstrated on histochemistry with periodic acid-Schiff stain after diastase digestion and with mucicarmine. CK7 and CK19 are usually highlighted with immunostaining, whereas CD56 is negative. CLC includes populations of small cells with a high nuclear: cytoplasmic ratio and hyperchromatic, oval nuclei growing in a tubular, cord-like, anastomosing pattern (“antler-like” pattern). These cells are embedded in a fibrous stroma and appear

to originate from the canals of Hering or cholangioles. These tumor cells may be immunohistochemically positive for CK19, KIT, CD56 (NCAM), and EpCAM. Cellular atypia is usually mild and mucin production is absent. HCC-like areas are frequently present at the periphery of the tumors, where the tumor cords are continuous with non-tumoral liver-cell cords in a replacing pattern of growth.<sup>2</sup> Typical histopathological images of CC and CLC are shown in Figures 1 and 2, respectively.

Pure-type CLC (CLC component >80%) can be distinguished from CC on the basis of detailed imaging findings, including evaluation with dynamic computed tomography (CT) or angiography-assisted CT, as reported by Kozaka et al.<sup>9</sup> Kozaka et al. summarized the characteristic findings of pure CLC as follows: intermingled portal venules in the tumor, tumoral staining in the arterial dominant phase (AP) with prolonged enhancement in the portal dominant phase (PP) to equilibrium phase (EP) of dynamic CT, ring-like or wedge-shaped peritumoral enhancement in the AP, and rare intrahepatic bile duct dilatation. We attributed these findings to cancer cell nests interspersed with abundant fibrous stroma and to the possible early drainage of contrast medium from the intratumoral blood sinusoids via abundant communications between the surrounding hepatic sinusoids and intermingled portal venules resulting from the replacing growth feature of pure CLC. These imaging features differ from those of CC, which demonstrates no definite staining in the AP.

Detailed immunohistological evaluation of resected ChC and CC specimens showed that SC-typical, SC-INT, CLC, and CC components are well mixed,<sup>7</sup> and their pathological features are complicated. Although it is important to consider how to discriminate between ChC and CC from histopathological images of resected specimens, the most important aspect for surgeons is how to assess the biological behavior of the tumor accurately based on preoperative imaging, to allow selection of an appropriate surgical procedure. If tumor malignancy could be evaluated accurately from preoperative imaging, it would be possible to provide the optimal surgical treatment, thus avoiding the excessive invasion of over-operation and deterioration resulting from under-operation. Accurate preoperative evaluation of the biological behavior of malignant tumors with

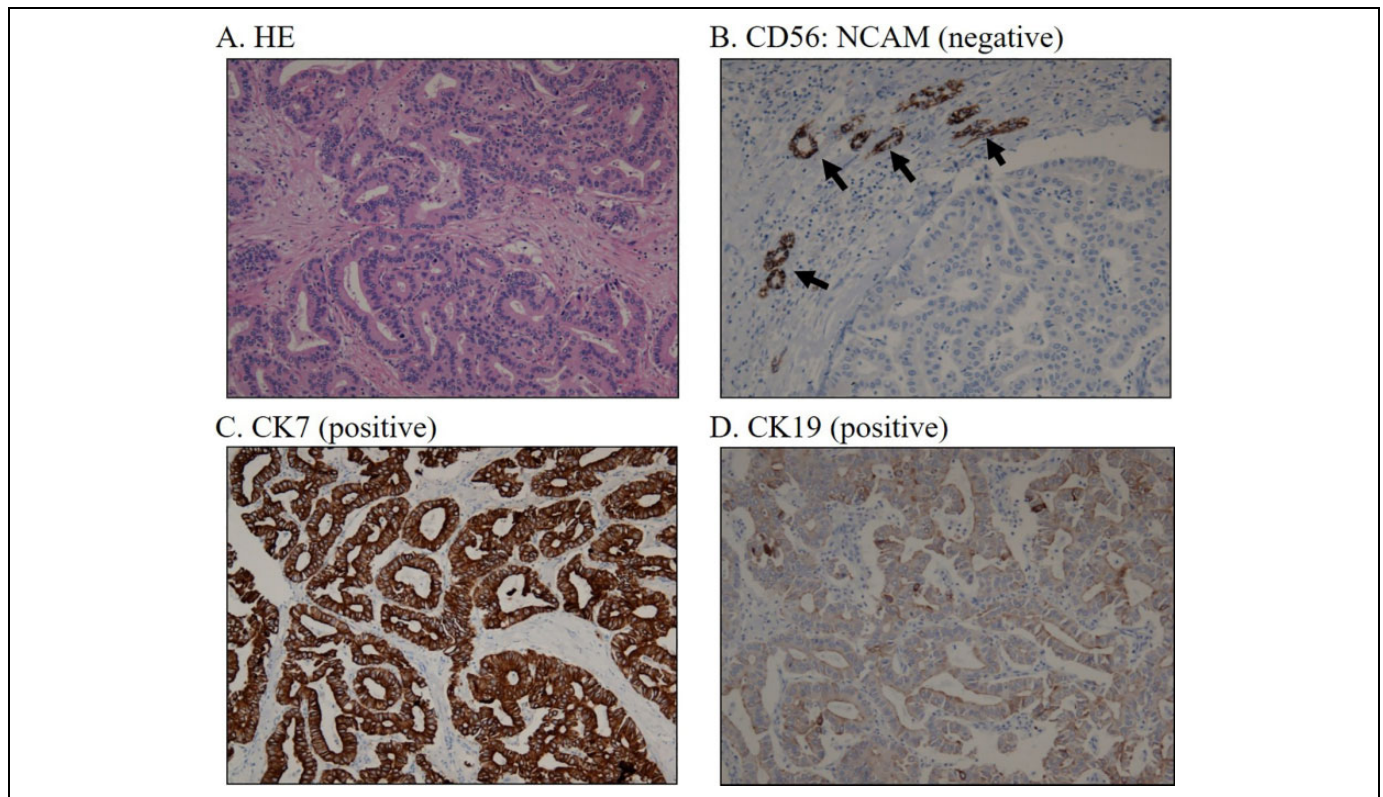


**Figure 1.** Immunohistochemical pathology of CC. A: Hematoxylin–eosin staining. B: CD56 immunohistochemical staining. Tumor area is negative for CD56, whereas the normal bile ductule (black arrows) surrounding the tumor is clearly stained with CD56. C: CK7 immunohistochemical staining. CK7 is strongly positive in the tumor area. D: CK19 immunohistochemical staining. CK19 is strongly positive in the tumor area. Tumor cells are typical adenocarcinoma, well-, moderately, or poorly differentiated, often accompanied by abundant stroma. There is mucin production and tumor cells were usually immunohistochemically positive for CK7 and CK19, but negative for NCAM (CD56) and HepPar1. Abbreviations: CC, cholangiocarcinoma; ChC, combined hepatocellular and cholangiocarcinoma; CK, cytokeratin; CLC, cholangiolocellular carcinoma; HepPar1, hepatocyte paraffin 1; NCAM, neural cell adhesion molecule.

diagnostic imaging thus offers important patient benefits. We therefore reevaluated cholangiocytic primary liver cancers from the viewpoint of the surgeon by evaluating the preoperative diagnostic imaging, pathological features, and surgical prognosis of HCC, CC, and ChC, including CLC. In particular, we clarified whether CLC should be evaluated as SC-type ChC or as a subtype of CC from the surgeon's perspective. Because angiography-assisted CT can provide a more precise differential diagnosis in patients with primary liver cancer, we performed angiography-assisted CT in addition to dynamic CT and gadolinium-ethoxybenzyl-diethylenetriamine-pentaacetic acid magnetic resonance imaging. We therefore emphasize the usefulness of angiography-assisted CT. In recent years, we have also used 18-fluoro-2-deoxyglucose positron-emission tomography (FDG-PET) in cases of suspected CLC or CC, and we discuss the value of this modality for evaluating the malignant potential of cholangiocytic primary liver cancers.

## Materials and Methods

The study subjects included 7 patients with classical type CHC, 8 with SC-INT type CHC, 13 with CLC type CHC, and 58 with

mass-forming-type CC. All patients underwent hepatectomy or living-related donor liver transplantation (LDLT) from 2001 to 2014. An additional 329 patients with hepatocellular carcinoma (HCC) who underwent hepatectomy or LDLT during the same period were included. Briefly, patients underwent hepatectomy, with the choice of resection based on tumor size, tumor location, preoperative diagnosis, and liver function. Patients with a preoperative diagnosis of HCC or ChC underwent hepatectomy without lymph node dissection, and patients with a preoperative diagnosis of CC or combined CLC and CC received hepatectomy with lymph node dissection (around the hepatoduodenal ligament, the common hepatic artery, or behind the pancreas head). Extrahepatic bile duct resection and reconstruction were performed if the tumor involved the bile duct in the perihilar region. The analysis of clinical data and use of resected specimens for immunohistological study were approved by the Kanazawa University Ethics Committee and informed consent was obtained from all individual patients included in this study.

Histological evaluation was performed by experienced pathologists (H.I., Y.S., M.S., K.H., and Y.N.). Immunological staining for cytokeratin (CK) 7, CK19, CD56 (neural cell

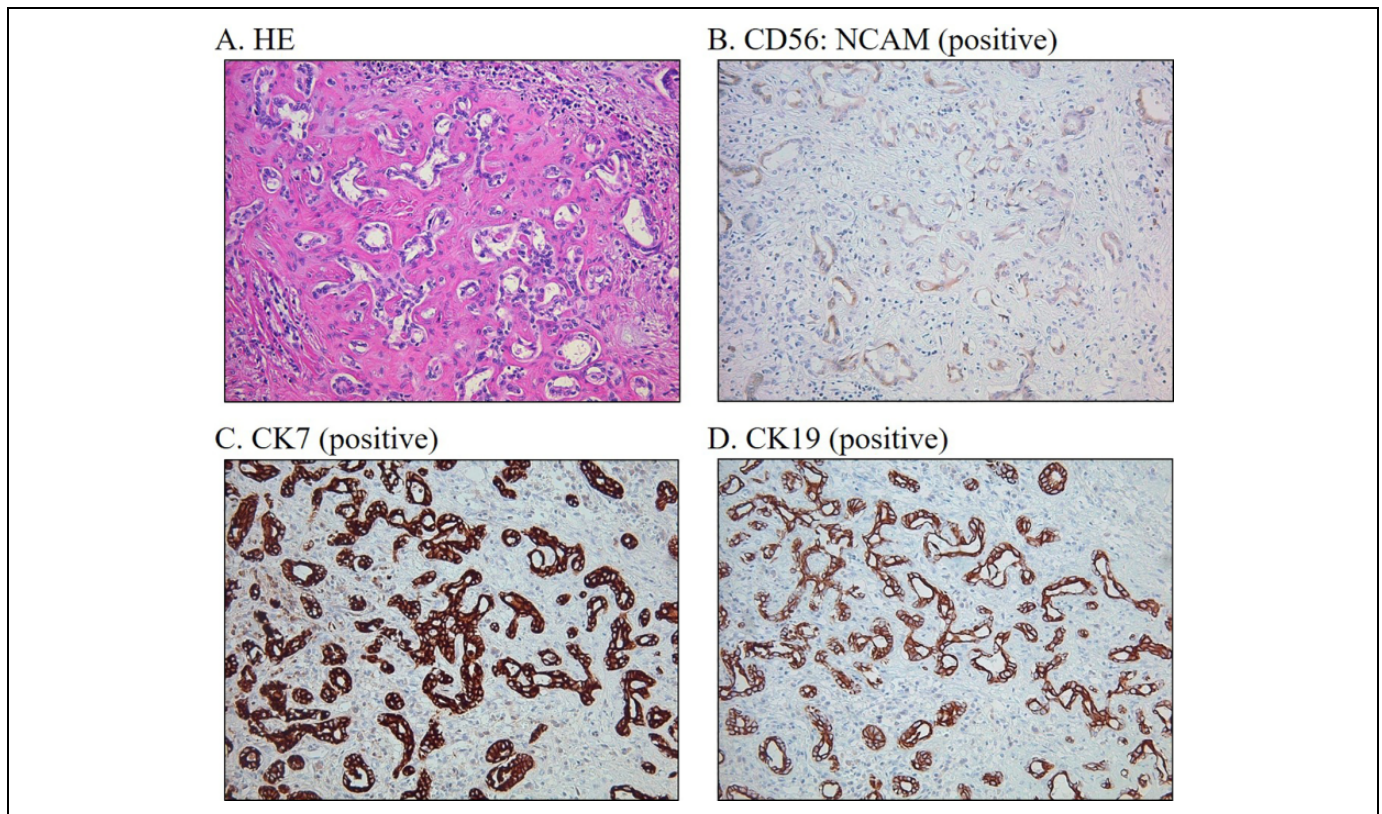


**Figure 2.** Immunohistochemical pathology of CLC. A: Hematoxylin–eosin staining. B: CD56 immunohistochemical staining. The tumor area is positive for CD56. C: CK7 immunohistochemical staining. CK7 is strongly positive in the tumor area. D: CK19 immunohistochemical staining. CK19 is strongly positive in the tumor area. Tumor cells are arranged in a tubular, cord-like, “antler-like” pattern with marked fibrous stroma. The tumor cords are continuous with the non-tumoral liver-cell cords in a replacing growth pattern. There is no mucin production and the tumor cells are usually immunohistochemically positive for CK7 and CK19, negative for HepPar1, and have a frequently positive but variable reaction for NCAM (CD56). Abbreviations: CC, cholangiocarcinoma; ChC, combined hepatocellular and cholangiocarcinoma; CK, cytokeratin; CLC, cholangiolocellular carcinoma; HepPar1, hepatocyte paraffin 1; NCAM, neural cell adhesion molecule.

adhesion molecule: NCAM), epithelial membrane antigen (EMA), epithelial cell adhesion molecule (EpCAM),  $\alpha$ -feto-protein (AFP), and hepatocyte-specific antigen (HepPar1) was also performed, except for tumors definitely diagnosed as HCC or CC. ChC subtype was diagnosed according to the WHO classification<sup>1</sup> (Table S1). In particular, CLC was defined as consisting of small tubular, acinar, or cord-like carcinoma cells resembling proliferating reactive bile ductules with internal HCC-like and CC areas, as described in the first report of CLC by Steiner & Higginson (1959).<sup>11</sup> CLC has been defined as a tumor in which the bile ductular component occupies >80% of the whole tumor,<sup>10</sup> but we defined the CLC component as significant at >50%.

All specimens were stained with hematoxylin and eosin, Gomori’s reticulin silver, and elastica van Gieson (EVG), and the growth pattern of the cancer cells at the border with the surrounding liver, the distribution of tumor cells in combination with interstitial fibrotic stroma, and necrosis were assessed. The presence/absence of portal venous invasion and internal portal tract were also evaluated.

Classical type ChC was defined as a mix of HCC, CC, and/or CLC with at least 10% of each; cases with <10% HCC were

defined as CC. No tumors were clearly diagnosed as SC-typical in this study. Tumors diagnosed as SC-INT showed no HCC component, but CLC and CC components were present. Tumors in which the SC-INT component was clearly identified were classified as SC-INT, regardless of the area occupied by SC-INT.

CK7, CK19, EMA, MUC1, EpCAM, CD56 (NCAM), AFP, and HepPar1 were examined with immunostaining, as described previously.<sup>7</sup> HepPar1 and AFP were used as hepatocellular or HCC markers; CK7, CK19, EMA, MUC1, and EpCAM as biliary epithelial markers; and CD56 (NCAM) as a hepatic progenitor cell marker. The primary antibodies used were as described previously.<sup>7</sup> In brief, sections were pre-treated with 0.05 M citric acid buffer (pH 6) at 95°C for 20 min in a microwave oven for antigen retrieval. After blocking endogenous peroxidase, the sections were incubated with the primary antibody at 4°C overnight. Envision+ solution (Dako, Santa Clara, CA, USA) was then applied for 30 min at room temperature and the reaction products were visualized with 3-3'-diaminobenzidine tetrahydrochloride (Sigma Chemical, Co., St. Louis, MO, USA) and H<sub>2</sub>O<sub>2</sub>. The sections were then lightly counterstained with hematoxylin. A similar dilution of

control mouse or rabbit IgG (Dako) was applied instead of the primary antibody as a negative control. Positive and negative controls were routinely included.

The prevalence and proportion of each component (HCC, INT, CLC, and CC) were assessed histologically according to the WHO classification (Table S1), together with the results of mucin staining and immunohistochemical staining for CK7, CK19, EMA, EpCAM, CD56 (NCAM), AFP, and HepPar1. Mucin staining was used to detect the CC component. The histological diversity score was defined as the number of histological components (HCC, INT, CLC, and CC) present in each tumor (score 1–5). HCC was classified as well-, moderately, or poorly differentiated, based on histological tumor differentiation.<sup>1</sup>

Angiography was performed after obtaining written informed consent from the patients. Angiography-assisted CT was also performed to analyze the hemodynamic characteristics of the lesions. After hepatic angiography, CT arterial portography (CTAP) and CT hepatic arteriography (CTHA) were performed with Xvision/SP or Aquilion64 (Toshiba Medical Systems, Tokyo, Japan). After femoral artery puncture, a 4-F catheter was selectively placed in the superior mesenteric artery for CTAP and in the common or proper hepatic artery for CTHA. CTAP scans were obtained at a section thickness of 5 to 7 mm, collimation of 5 to 7 mm, and reconstruction intervals of 2.5 mm, covering the entire liver in a single breath-hold. Helical CT scanning began 25 s after starting infusion of 50 to 70 mL iohexol (320–350 mgI/mL, Omnipaque; Daiichi Sankyo, Tokyo, Japan) at a rate of 1.8 mL/s via a power injector. Prostaglandin E1 (5 mg; Palux; Taisho, Tokyo, Japan) was injected into the superior mesenteric artery before contrast material infusion to increase the blood flow and decrease the laminar flow of the portal vein. Approximately 10 min after CTAP, CTHA scans were obtained at a section thickness of 3 to 5 mm, collimation of 3 to 5 mm, and reconstruction intervals of 1.5 to 2.5 mm. CTHA scanning began 7 s (early phase) and 60 s (delayed phase) after starting injection of iohexol into the common/proper hepatic artery at a rate of 1.8 mL/s. The infusion was continued throughout the early-phase scanning. The radiological characteristics and hemodynamics of the lesion were further assessed with single-level dynamic CTHA by infusing 10 mL of contrast material into the common hepatic artery at a rate of 1.0 mL/s via a power injector. Scanning began immediately prior to dye injection and was performed with 3-mm slices during a single breath-hold, using a 40-s continuous technique (220 mA, 120 kVp). High-resolution images of the lesions were reconstructed at 1-s intervals using a small field of view.

Tumor staining on early-phase CTHA was classified as positive (homogeneous, inhomogeneous, or peripheral staining) or negative enhancement. Hyperattenuation relative to the surrounding liver, except in the area with peritumoral enhancement, was defined as positive enhancement. Delayed tumoral enhancement was classified as either positive or negative prolonged staining, as described in the equilibrium phase (EP) of the dynamic CT evaluation section. The pattern of peritumoral enhancement in the early phase of CTHA was classified as

ring-like, corona-like, or wedge-shaped, as also described in the artery dominant phase (AP) of the dynamic CT evaluation section. Continuous hemodynamic changes in pure CLC were analyzed with single-level dynamic CTHA, and the images were assessed with special attention paid to both tumoral and peritumoral enhancement and intratumoral vasculature. The intratumoral portal blood supply and/or portal tracts inside the tumor were also evaluated. Angiographic procedures were performed by radiologists (K.K., K.K., T.G., and O.M.) who each have >8 years of experience performing abdominal angiography.

Semiquantitative analysis of 18F-FDG uptake and maximum standardized uptake values (SUVmax) of the tumors were interpreted in PET images by a radiologist specializing in nuclear medicine.

The histopathological stage of the resected specimens was evaluated according to the 6th edition of The General Rules for the Clinical and Pathological Study of Primary Liver Cancer by the Liver Cancer Study Group of Japan (Kanehara & Co., Ltd., July 2015). Briefly, stage IV was defined as either lymph node metastasis-positive (N1) or distant organ metastasis-positive (M1), regardless of T factor, or T4 without lymph node metastasis or distant organ metastasis (T4 is >2-cm diameter with vascular invasion and intrahepatic metastasis).

Numerical data are presented as mean  $\pm$  standard deviation and were compared with Student's *t*-test or Welch's *t*-test. Correlations between 2 factors were evaluated with the  $\chi^2$  test. Overall survival and progression-free survival were compared with log-rank tests with the Kaplan–Meier method, and multivariate analysis of overall survival was conducted using Cox's proportional hazard model with IBM SPSS Statistics software (IBM Japan). A *p* value < 0.05 was considered significant.

## Results

Details of the study patients are described in Table 1.

### Sample Case Demonstrating the Origins of CLC

We present the details of a sample case demonstrating the possible origin of CLC. This patient suffered from glycogen storage disease type 1a and had combined CLC and CC. Although glycogen storage disease type 1a is a frequent complication of primary liver tumors,<sup>12</sup> there have been no previous reports of the condition in conjunction with CLC. As shown in Figure 1, this patient had a large hypovascular liver tumor accompanied by infiltration of the hepatic hilum. High accumulation on FDG-PET CT and suspected extrahepatic lymph node metastasis led to an initial diagnosis of CC. CTAP of angiography-assisted CT revealed a perfusion defect (Figure 3A), but intratumoral portal vein penetration was also observed (Figure 3B). CTHA showed intratumoral arterial penetration (Figure 1C) and tumor infiltration of the hepatic hilum (Figure 3D). Furthermore, lymph node metastasis was observed in contact with the proper hepatic artery (Figure 3E). FDG-PET showed an SUVmax of 11.7 in the early phase and

**Table 1.** Clinicopathological Features of Patients With ChC, CC, and HCC.

Histology		HCC (n = 329)	Classic (n = 7)	SC-INT (n = 8)	CLC (n = 13)	CC (n = 58)
Age: years (mean ± SD)		64 ± 10 <sup>#1</sup>	65 ± 7	59 ± 12 <sup>#1</sup>	72 ± 10 <sup>#1</sup>	62 ± 10 <sup>#1</sup>
Gender: female		73 (22.2%) <sup>#1</sup>	2 (28.1%)	2 (25.0%)	5 (38.5%)	24 (41.4%) <sup>*1</sup>
Background liver disease						
HBV		91 (27.7%)	3 (42.9%)	3 (37.5%)	2 (15.4%)	8 (13.8%)
HBV & HCV		3 (0.9%)	0	0	0	0
HCV		148 (45.0%) <sup>#1</sup>	1 (14.3%)	2 (25%)	4 (30.8%)	4 (6.9%) <sup>*1</sup>
Background liver cirrhosis		163 (49.7%) <sup>**1</sup>	5 (71.9%) <sup>**1</sup>	6 (75%) <sup>**1</sup>	1 (7.7%) <sup>##1</sup>	7 (12.1%) <sup>##1</sup>
AFP: ng/mL (mean ± SD)		4971.8 ± 33041.1 <sup>**1,2</sup>	44.4 ± 49.1 <sup>**1</sup>	670.5 ± 1404.6 <sup>**1</sup>	31.2 ± 60.8 <sup>##2</sup>	7.5 ± 22.3 <sup>##1</sup>
PIVKA-II: mAU/mL (mean ± SD)		2949.1 ± 12584.4 <sup>**1</sup>	54.7 ± 50.5 <sup>##1</sup>	287.4 ± 702.6 <sup>##1</sup>	77.6 ± 195.1 <sup>##1</sup>	114.2 ± 463.2 <sup>##1</sup>
CEA ng/mL (mean ± SD)		3.2 ± 1.7 <sup>##1</sup>	3.3 ± 1.5	2.7 ± 1.3	2.9 ± 1.9	22.5 ± 57.1 <sup>**1</sup>
CA19-9: ng/mL (mean ± SD)		40.0 ± 185.6 <sup>##1</sup>	10.0 ± 12.8	48.3 ± 78.4	36.9 ± 32.7	2549.4 ± 8495.5 <sup>**1</sup>
Surgical procedure						
Non-anatomical						
Anatomical						
LDLT		127 (38.6%)	4 (57.1%)	1 (12.5%)	5 (38.5%)	5 (8.6%)
Pre-operative treatment (RFA, TAE, TACE)		182 (55.3%) <sup>#1</sup>	2 (28.6%) <sup>#1</sup>	5 (62.5%) <sup>#1</sup>	8 (61.5%) <sup>#1</sup>	53 (91.4%) <sup>*1</sup>
Tumor size: mm (mean ± SD)		20 (6.1%)	1 (14.3%)	2 (25.0%)	0	0
Intrahepatic metastasis (+)		57 (17.3%) <sup>#1,*2</sup>	2 (28.6%) <sup>*2</sup>	4 (50%) <sup>*1</sup>	1 (7.7%) <sup>#1</sup>	0 <sup>#1,2</sup>
Vp ≥ 2 or Vv ≥ 2		44.1 ± 30.3 <sup>##1,**3</sup>	25.0 ± 5.2 <sup>##1,2,3</sup>	50.0 ± 25.9 <sup>**2</sup>	33.4 ± 16.3 <sup>##1,3</sup>	59.0 ± 30.7 <sup>**1</sup>
B ≥ 2		56 (17.0%) <sup>#1</sup>	1 (14.3%)	4 (50%) <sup>*1</sup>	2 (15.4%)	19 (32.8%) <sup>*1</sup>
Stage I~III		28 (8.5%) <sup>#1</sup>	0 <sup>#1</sup>	1 (12.5%)	1 (7.7%) <sup>#1</sup>	27 (46.6%) <sup>*1</sup>
IV		6 (1.8%) <sup>#1,2</sup>	0 <sup>#1</sup>	0 <sup>#1</sup>	2 (15.4%) <sup>*2</sup>	23 (39.7%) <sup>*1</sup>
N (+)		250 (76.0%)	7 (100%)	4 (50%)	10 (76.9%)	20 (34.5%)
CLC component (+)		79 (24.0%) <sup>#1</sup>	0 <sup>#1</sup>	4 (50%)	3 (23.1%) <sup>#1</sup>	38 (65.5%) <sup>*1</sup>
Mucin production (+)		8 (2.4%) <sup>#1</sup>	0 <sup>#1</sup>	1 (12.5%) <sup>#1</sup>	2 (15.4%) <sup>#1</sup>	31 (53.4%) <sup>*1</sup>
Positive rate of peritumoral bile duct dilatation by CT study		0 <sup>#12</sup>	1 (14.3%) <sup>#1,*2</sup>	2 (25%) <sup>#1,*2</sup>	13 (100%) <sup>*1</sup>	3 (5.2%) <sup>#1,*2</sup>
Positive rate of intratumoral portal vein or hepatic vein penetration by CT study		0 <sup>#12</sup>	4 (57.1%) <sup>#1,*2</sup>	4 (50%) <sup>#1,*2</sup>	4 (30.8%) <sup>#1,*2</sup>	54 (93.1%) <sup>*1</sup>
Positive prolonged stain by CT study		6 (1.8%) <sup>#1</sup>	0 <sup>#1</sup>	0 <sup>#1</sup>	1 (7.7%) <sup>#1</sup>	33 (56.9%) <sup>*1</sup>
Early enhancement and early wash out with corona-like stain by CT study		0 <sup>#1</sup>	0 <sup>#1</sup>	0 <sup>#1</sup>	9 (69.2%) <sup>*1</sup>	0 <sup>#1</sup>
No enhancement area in the tumor by delayed phase of CT study <sup>1)</sup>		85 (25.8%) <sup>#1</sup>	2 (28.6%) <sup>#1</sup>	1 (25%) <sup>#1</sup>	12 (92.3%) <sup>*1</sup>	42 (72.4%) <sup>*1</sup>
FDG-PET: SUV max (mean ± SD)		223 (68%) <sup>*1</sup>	4 (57.1%) <sup>*1</sup>	6 (75%) <sup>*1</sup>	1 (7.7%) <sup>#1</sup>	0 <sup>#1</sup>
Over-all survival rate (Number of survivors)		3 (0.9%) <sup>#1</sup>	1 (14.3%) <sup>#1</sup>	0 <sup>#1</sup>	0 <sup>#1</sup>	39 (67.2%) <sup>*1</sup>
3 years		NS	NS	NS	4.0 ± 3.7 <sup>##1</sup>	8.8 ± 5.4 <sup>**1</sup>
5 years						
10 years						
Recurrent rate (number of survivors)						
3 years		HCC <sup>**1</sup>	Classic <sup>**1</sup>	SC-INT <sup>##1</sup>	CLC <sup>**1</sup>	CC <sup>##1</sup>
5 years		84.1% (255)	100% (7)	50% (4)	92.3% (12)	38.6% (22)
10 years		79.0% (229)	83.3% (6)	37.5% (2)	84.6% (9)	30.9% (12)
		72.5% (94)	83.3% (4)	18.8% (1)	84.6% (2)	30.9% (7)
		HCC <sup>##1,**2</sup>	Classic	SC-INT <sup>##1</sup>	CLC <sup>**1</sup>	CC <sup>##1,2</sup>
3 years		44.7% (132)	57.1% (4)	25% (2)	76.9% (10)	25.7% (13)
5 years		39.8% (110)	28.6% (2)	25% (2)	59.8% (7)	25.7% (9)
10 years		36.6% (46)	28.6% (1)	25% (1)	59.8% (2)	22.5% (6)

(continued)

**Table 1. (continued)**

Histology		HCC (n = 329)	Classic (n = 7)	SC-INT (n = 8)	CLC (n = 13)	CC (n = 58)
Factors						
First (early) recurrent site						
No recurrence	134 (40.7%)* <sup>1</sup>	2 (28.6%)	2 (25%)	8 (61.5%)* <sup>1</sup>	13 (22.4%)* <sup>1</sup>	
Local recurrence	6 (1.8%)	0	0	0	4 (6.9%)	
Intrahepatic metastasis	171 (52%)* <sup>1</sup>	4 (57.1%)	6 (75%)	4 (30.8%)	29 (50%)* <sup>1</sup>	
Lymph node metastasis	3 (0.9%)	0	0	1 (7.7%)	2 (3.4%)	
Peritoneal dissemination	3 (0.9%)* <sup>1</sup>	1 (14.3%)	0	0	7 (12%)* <sup>1</sup>	
Lung metastasis	4 (1.2%)	0	0	0	2 (3.4%)	
Bone metastasis	5 (1.5%)	0	0	0	3 (5.2%)	

<sup>1</sup>) Excluding cystic degeneration and hemorrhage in the tumor.

In  $\chi^2$  tests, \*1 and \*2 were significantly higher than #1 and #2, respectively ( $p < 0.05$ ).

In Student's and Welch's *t*-tests, \*\*1, \*\*2, and \*\*3 were significantly higher than #1, #2, and #3, respectively ( $p < 0.05$ ).

In log-rank tests, \*\*\*1 and \*\*\*2 were significantly higher than ##1 and ##2, respectively ( $p < 0.05$ ).

Stage was evaluated according to the 6th edition (July 2015) of The General Rules for the Clinical and Pathological Study of Primary Liver Cancer established by the Liver Cancer Study Group of Japan (Kanehara Shuppan, Tokyo, Japan, 2015).

Abbreviations: AFP, alpha-fetoprotein; B  $\geq$ , tumor invasion observed in 2 or more intrahepatic bile ducts (Liver Cancer Study Group of Japan 2015); CA19-9, carbohydrate antigen 19-9; CC, cholangiocellular carcinoma; CE/A, carcinoembryonic antigen; ChC, combined hepatocellular and cholangiocarcinoma; Classic, classical type ChC; CLC, cholangiocellular carcinoma (ChC SC subtype); FDG-PET SUV max, <sup>18</sup>F-fluoro-2-deoxy-d-glucose protein emission tomography standardized uptake maximum value; HCC, hepatocellular carcinoma; LDLT, living-related donor liver transplantation; N(+), positive lymph node metastasis; PIVKA-II, protein induced by vitamin K antagonist or absence-II; RFA, radiofrequency ablation therapy for tumor; SC-INT, intermediate cell subtype of ChC with stem cell features (ChC SC subtype); TACE, transcatheter arterial chemoembolization therapy for tumor; TAE, transcatheter arterial embolization therapy for tumor; Vp  $\geq$ 2, tumor invasion in 2 or more branches of the portal vein (Liver Cancer Study Group of Japan 2015); Vv  $\geq$ v, tumor invasion in 2 or more branches of the hepatic vein (Liver Cancer Study Group of Japan 2015).

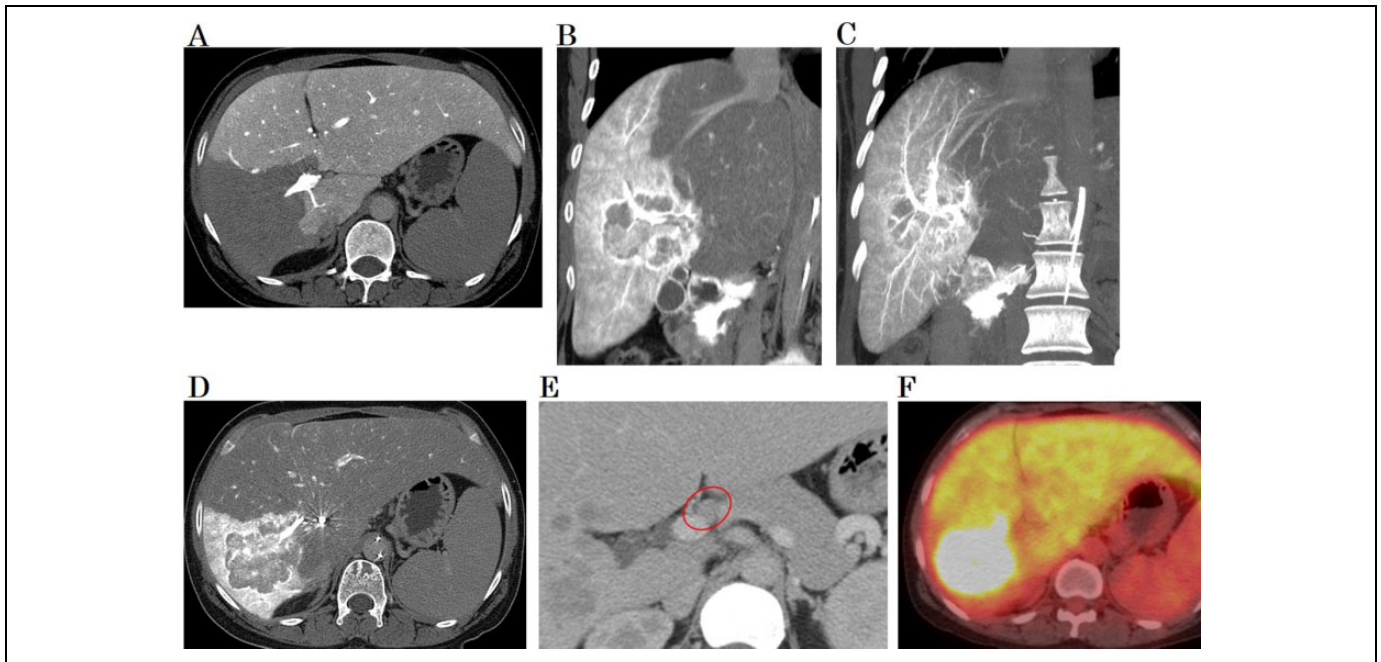


**Figure 3.** Images of a complex CLC with various histopathological features, including CC and HCC components. The patient had glycogen storage disease type 1a and a large tumor, but intratumoral Glisson's pedicle penetration (specific for CLC) and no peripheral intrahepatic bile duct dilatation on angiography-assisted CT. A: Tumor portal venous perfusion defect observed with CTAP, despite intra-tumoral portal vein penetration, which was specific for CLC, including CC component extension to hepatic hilum. B: Intra-tumoral portal vein penetration observed with CTAP. C: Intra-tumoral hepatic arterial penetration observed with CTHA. D: Tumor progression to hepatic hilum observed with CTHA. E: Metastatic lymph node in contact with proper hepatic artery. F: FDG-PET/CT in delayed phase. The SUVmax of the tumor was high (early-phase 11.7, delayed phase 12.8). Two intrahepatic metastatic lesions also showed extremely high uptake, but no uptake was found in the lymph node metastatic lesion. Abbreviations: CC, cholangiocarcinoma; CLC, cholangiolocellular carcinoma; CT, computed tomography; CTAP, CT during arterial portography; CTHA, CT during hepatic arteriography; FDG-PET, 18-fluoro-2-deoxyglucose positron-emission tomography; HCC, hepatocellular carcinoma; SUV, standardized uptake value.

12.8 in the delayed phase (Figure 3F). The initial diagnosis based on preoperative imaging was CC with invasion of the hepatic hilum and extrahepatic lymph node metastasis; however, there was intratumoral penetration of Glisson's pedicle and no dilatation of the bile ducts peripheral to the tumor, despite the large size of the tumor. The consequent diagnosis was CLC, in which the infiltration at the hepatic hilum was replaced by CC. The patient underwent right hemihepatectomy with extrahepatic bile duct resection, biliary reconstruction, and extrahepatic lymph node dissection.

The histopathological features of the resected specimen are shown in Figure 4A. The tumor margin was HCC-like, with a trabecular or pseudoglandular construction (Figure 4B). The margin was positive for AFP (Figure 4C) but negative for HepPar1, indicating a diagnosis of intermediate type between HCC and CLC. In contrast, the most extensive part of the lesion was typical CLC (Figure 4D) and was focally positive for CD56 (NCAM) (Figure 4E) and diffusely positive for both CK7 and CK19 (Figure 4F, 4G). The hepatic hilum-infiltrating lesion was mainly CC component, similar to the large bile duct and the perineural invasion (Figure 4H), intrahepatic metastasis (Figure 4I), and lymph node metastasis (Figure 4J). Both AFP and CD56 were negative. Although CLC is derived from cells with the ability to differentiate into both

hepatocytes and cholangiocytes,<sup>4,13</sup> the finding that the tumor in this case transitioned to the CC component near the hepatic hilum indicates that CLC is essentially a tumor on the differentiation pathway to CC. These observations suggest that CLC should be clinically classified as a subtype of CC, rather than as a subtype of ChC.

### Clinicopathological Findings of ChC and Combined-Type CC

The relative areas occupied by the different histological components based on the largest split surface of 32 tumors diagnosed as ChC or CC mixed with other histological components are shown in Figure 5. Experienced pathologists diagnosed Cases 1 through 7 as classical ChC, Cases 8 through 15 as SC-INT subtype, Cases 16 through 28 as CLC subtype, and Cases 29 through 32 as CC. Most cholangiocyte tumor components of classical ChC were CC components, with mixed CLC components in only 1 case. Five of the 8 cases (62.5%) of SC-INT had CLC or CC components. Among the 13 tumors diagnosed as CLC, CC components were detected in 7. SC-INT components were observed in 1 case, but no HepPar1-positive HCC component was observed. In patients 16 and 27, who died of cancer-related causes, the progressive



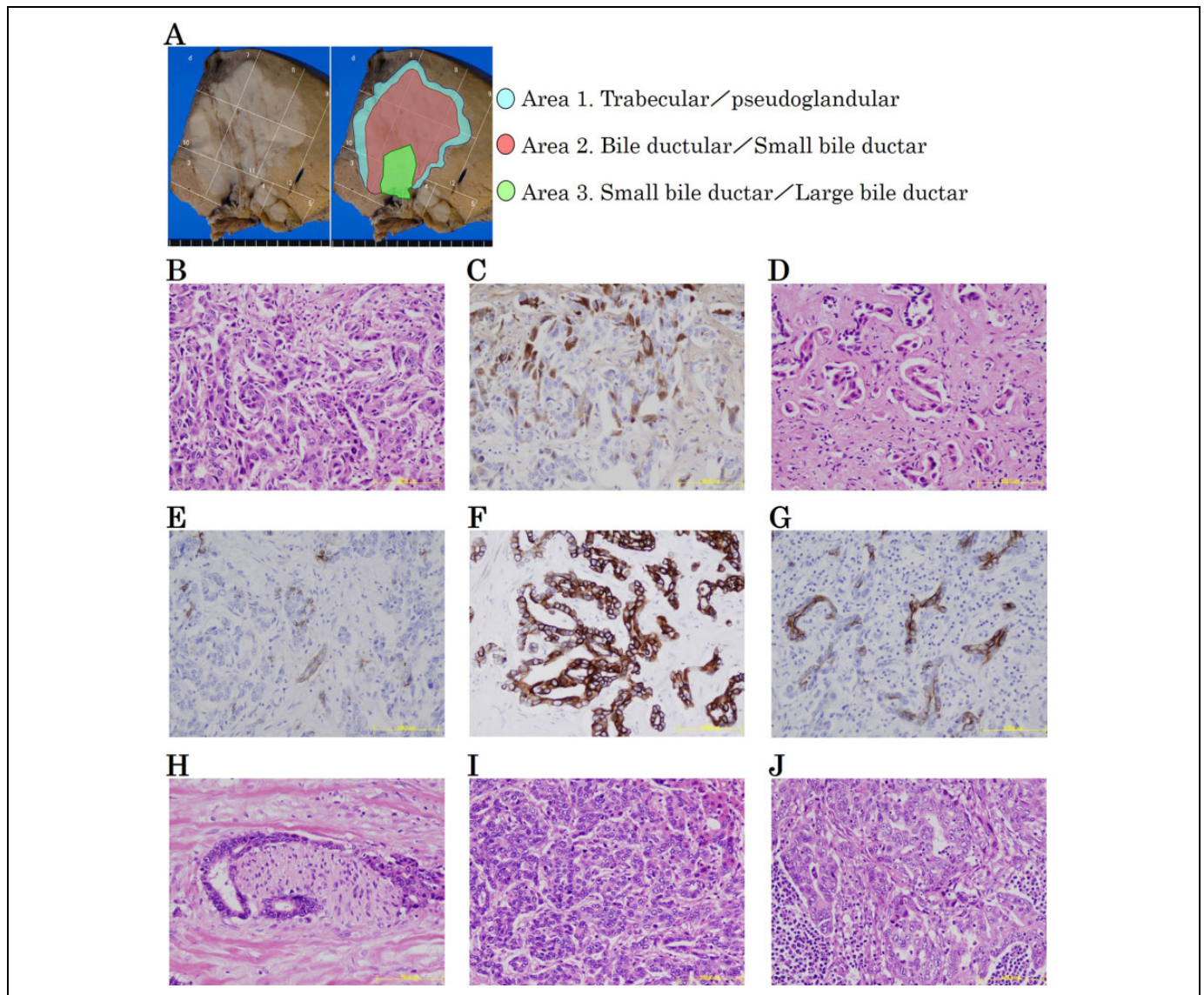


**Figure 4.** Patient with glycogen storage disease type 1a and CLC with various histopathological features, including CC and HCC components. A: HCC-like components such as trabecular/pseudoglandular features (area 1) are seen in the tumor marginal region with replacement growth. The intratumoral central lesion (area 2) has CLC features, and CC features are seen in the invasive lesion at the hepatic hilum (area 3), with periductal invasion, perineural invasion, and lymph node metastases (pStage IVA\*). B: Hematoxylin–eosin staining of peripheral trabecular/pseudoglandular HCC-like SC-INT component (see also Figure 2A, area 1). C: AFP immunohistochemical staining of peripheral trabecular/pseudoglandular HCC-like SC-INT component (see also Figure 4A, area 1), which was AFP-positive but HepPar1-negative. D: Hematoxylin–eosin staining of central CLC component (see also Figure 4A, area 2). Tumor cells are arranged in a tubular, cord-like, “antler-like” pattern with marked fibrous stroma. The tumor cords are continuous with the non-tumoral liver cell cords in a replacing growth pattern. There is no mucin production. E: CD56 immunohistochemical staining of central CLC component (see also Figure 4A, area 2). The area is positive for CD56. F: CK7 immunohistochemical staining of CLC component (see also Figure 4A, area 2). CK7 is strongly positive in the tumor area. G: CK19 immunohistochemical staining of CLC component (see also Figure 4A, area 2). CK19 is strongly positive in the tumor area. H: Hematoxylin–eosin staining of hepatic hilar perineural invasive CC component (see also Figure 4A, area 3). I: Hematoxylin–eosin staining of intrahepatic metastasis of CC component (see also Figure 4A, area 3). J: Hematoxylin–eosin staining of lymph-node metastasis of CC component (see also Figure 4A, area 3). Abbreviations: CC, cholangiocarcinoma; ChC, combined hepatocellular and cholangiocarcinoma; CK, cytokeratin; CLC, cholangiolocellular carcinoma; HepPar1, hepatocyte paraffin 1; NCAM, neural cell adhesion molecule; SC-INT, intermediate cell subtype of ChC with stem cell features. \*General Rules for the Clinical and Pathological Study of Primary Liver Cancer, July 2015 (6th edition), Liver Cancer Study Group of Japan (Kanehara Shuppan, Tokyo, Japan).

lesion at the hepatic hilum was replaced with a CC component, with lymph node metastasis of the CC component. Case 27 had glycogen storage disease type 1a and is described in

detail above. Four patients with CC had CLC components present and 2 had a low percentage of HCC components. The above observations suggest that ChC can differentiate into

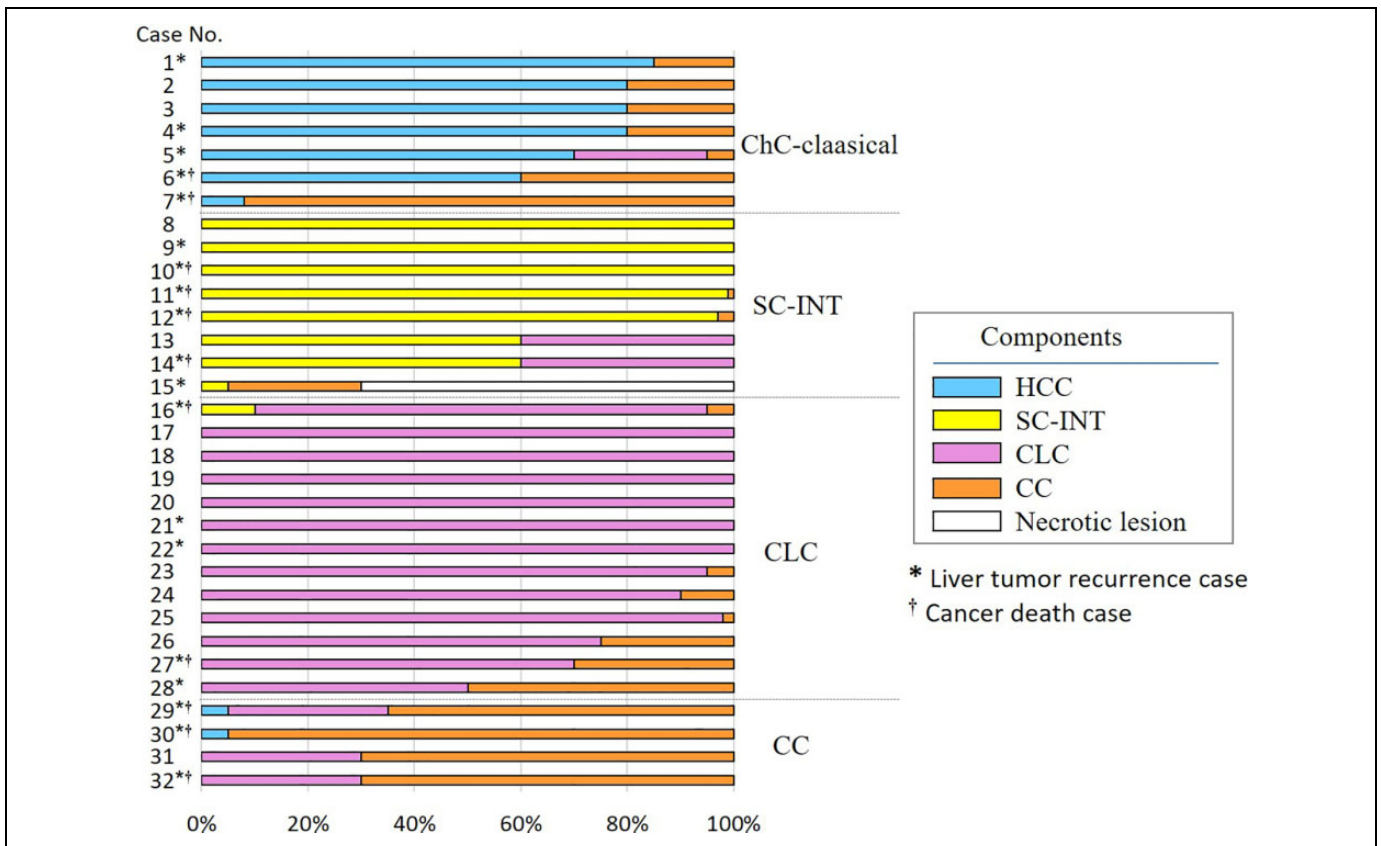


**Figure 5.** Relative prevalence of different pathological components in ChC and CC. Each component was present at various frequencies and was not always clearly distinguished. However, CLC was transformed to CC component with extension, whereas there was almost no clear mixture with HCC components. CLC thus appears to differentiate into CC, suggesting that CLC should be regarded as a subtype of CC. Abbreviations: CC, cholangiocarcinoma; ChC, combined hepatocellular and cholangiocarcinoma; CLC, cholangiolocellular carcinoma; HCC, hepatocellular carcinoma; SC-INT, intermediate cell subtype of ChC with stem cell features.

both hepatocytes and cholangiocytes,<sup>4,13</sup> whereas CLC tends to differentiate into cholangiocytes, as indicated by the fact that CLC transformed into CC component with progression to the hepatic hilum, and lymph node metastasis was also the CC component. CLC should thus be regarded clinically as a peripheral subtype of CC with a good prognosis, rather than as a subtype of ChC.

### Preoperative Imaging Diagnosis by Angiography-Assisted CT

The classification of CLC as an independent subtype of CC rather than as a subtype of ChC is supported by the characteristic imaging findings of CLC. The detailed imaging findings of pure CLC have been described previously,<sup>9</sup> and the imaging and histopathological results for typical pure CLC cases are shown in Figures 3 and 6. In addition to perfusion defects on CTAP, clear intratumoral portal vein penetration was observed, with no dilatation of the peripheral bile duct (Figure 6A). The histopathology of pure CLC with EVG staining revealed replacement growth and normal Glisson's pedicle (Figure 6B). Perfusion defects on CTAP (Figure 6C) and intratumoral hepatic vein penetration (Figure 6D) were also

observed in another tumor with replacement growth and hepatic vein penetration. Demonstrable intratumoral Glisson's pedicle and hepatic vein penetration on CTHA and CTAP were specific imaging findings of CLCs of a certain size (Table 2), and all 4 other CLC cases in which no penetration was detected were small. Furthermore, CLC could easily be distinguished from HCC, other ChC subtypes, and CC by detailed evaluation of the contrast patterns on CTHA and CTAP, as noted previously.<sup>9</sup> These results suggest that angiography-assisted CT may be the most useful modality for determining operative procedures because of its ability to evaluate tumor histological type accurately. The characteristic findings of CLC can be summarized as intratumoral Glisson's pedicle and hepatic vein penetration without peripheral bile duct dilatation, tumoral staining in the AP and prolonged enhancement in the PP to EP on dynamic CT, and ring-like or wedge-shaped peritumoral enhancement in the AP.

### Preoperative FDG-PET

The preoperative FDG-PET images in patients with CLC and CC are shown in Figure 7. CLC had a lower SUVmax than CC, and FDG-PET may thus be a useful auxiliary diagnostic tool.

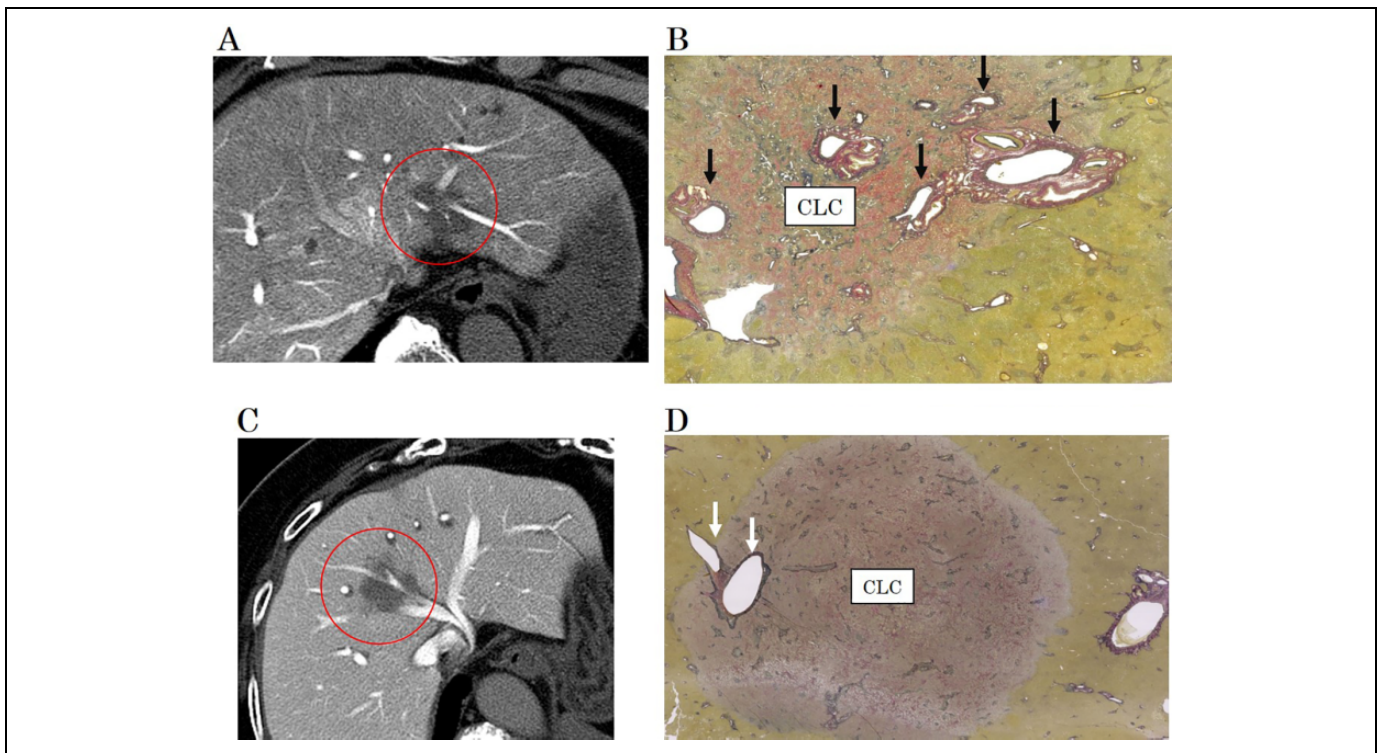


**Figure 6.** Replacement growth and penetration of the portal vein, hepatic artery, bile duct, and hepatic vein within CLC tumors. Tumor cells directly attach to the surrounding hepatocytes, with no compression against the surrounding liver. Hepatic supporting structures, such as the portal vein, hepatic vein, and bile duct, penetrate the tumor in CLC. A: Tumor portal vein penetration in CLC observed with CTAP. B: Microscopic image of Glisson's pedicle penetration of tumor (black arrows) in CLC with EVG staining. C: Tumor hepatic vein penetration in CLC observed with CTAP. D: Microscopic image of tumor hepatic vein penetration (white arrows) in CLC with EVG staining. Abbreviations: CLC, cholangiolocellular carcinoma; CT, computed tomography; CTAP, CT during arterial portography; CTHA, CT during hepatic arteriography; EVG, elastica van Gieson.

However, the SUVmax was very high in the above-mentioned case with hepatic hilar invasion and lymph node metastasis (Figure 7A). Excluding this unique case, the cut-off value for SUVmax for distinguishing between CLC and CC was estimated to be 4.23. When CLC and CC were evaluated together, the SUVmax of the primary tumor was significantly higher in cases with cancer recurrence than in those without recurrence.

### Surgical Prognosis

The prognoses for each tumor tissue type are compared in Figures 8 and 9. It was not possible to evaluate the prognosis for each stage of ChC because of the small number of cases; however, in a comparison of all cases with surgical resection, HCC, classical ChC, and CLC showed significantly better prognoses in terms of overall survival, compared with SC-INT and CC. As shown in Table 1, the prevalence of stage IV was significantly highest in CC, and that trend was also recognized in SC-INT. In contrast, CLC had a significantly lower incidence of recurrence than HCC, SC-INT, and CC, a finding associated with its relatively good prognosis. The recurrence rate of HCC was also significantly lower than that of CC. We inferred that the recurrence rates of HCC and classical ChC tumors were high because of the high rate of

multicentric recurrence, despite their having similar overall survival to that of CLC. However, CC recurrences were metastatic in all cases. In addition, as shown in Table 1, the better outcomes of CLC were presumed to be related to the lower frequency of liver cirrhosis and to the lower frequency of multicentric recurrence rate than that of HCC and classical ChC, despite the relatively high frequency of hepatitis C. The liver was the most common initial site of recurrence for all histological types; however, this included multicentric recurrence, and the relevance of this therefore varied among tissue types.

Because the number of cases of each CLC subtype was small and therefore we could not evaluate the prognosis for each stage, multivariate analysis using bivariates of stage and histological type was performed with Cox's proportional hazard model (Table 3). Organization type was divided into HCC, classical ChC, CLC with good prognosis, SC-INT, and CC with poor prognosis. Stage was evaluated separately for poor prognosis (stage IV) and relatively good prognosis (others), and histological type was evaluated as a significant prognostic factor independent of stage. Although it was not possible to evaluate the prognosis for each stage, this analysis demonstrated that histological type significantly affected the prognosis.

**Clinicopathological Features of ChC, CC, and HCC**

The clinicopathological features are summarized in Table 1. Patients with CLC were significantly older than patients with other types of tumors. The CC group included a higher proportion of women and had lower frequencies of hepatitis C and B, with a consequently lower frequency of liver cirrhosis. In contrast, although the frequency of hepatitis C was high among patients with CLC, the frequency of liver cirrhosis was significantly lower than that among patients with HCC, classical

ChC, or SC-INT, and was even lower than that among patients with CC. Preoperative tumor markers, including AFP, PIVKA-II, CEA, and CA19-9, tended to be lower in CLC, possibly reflecting the relatively low-grade malignancy of CLC. Both CEA and CA19-9 were significantly higher in CC than in other tumors, whereas AFP was significantly higher in HCC, classical ChC, and SC-INT; PIVKA-II was significantly higher in HCC. AFP and PIVKA-II may therefore be useful for discriminating between HCC and CLC. The frequency of anatomical hepatectomy was highest among CC patients, and hemi-hepatectomy, extrahepatic bile duct resection with biliary tract reconstruction, and lymph node dissection were also performed more frequently in CC patients.

**Table 2.** Distinction Between CLC and Other ChC Subtypes, HCC, and CC on Angiography-Assisted CT.

	Portal venous penetration
CLC (n = 13)	9 (69.2%)*
Other ChC subtype (n = 15)	0
HCC (n = 329)	0
CC (n = 58)	0

\* CLC significantly higher than other histological types according to  $\chi^2$  test ( $p < 0.05$ ).

Abbreviations: CC, cholangiocarcinoma; ChC, combined hepatocellular and cholangiocarcinoma; CLC, cholangiolocellular carcinoma; SC-INT, intermediate cell subtype of ChC with stem cell features; HCC, hepatocellular carcinoma.

It was possible to distinguish CLC from other ChC subtypes, HCC, and CC by evaluating hepatic structure penetration within the tumor. Intratumoral penetration by the portal vein, bile duct, and hepatic vein was a specific finding of CLC.

Half of the patients with SC-INT underwent preoperative treatments such as transcatheter arterial embolization or transcatheter arterial chemoembolization to prevent down-staging and rupture. Intrahepatic metastasis was significantly more frequent among patients with SC-INT and CC than among other groups, and was the main reason for the poor prognosis of these tumor types. Vascular and bile duct invasion were significantly more common in CC but were less common in CLC because of its replacing growth and intratumoral Glisson’s pedicle and hepatic vein penetration.

The CC group included a significantly higher proportion of patients with stage IV tumors because of the high frequency of lymph node metastasis. The frequency of stage IV tumors also tended to be high among SC-INT patients, reflecting the high frequency of intrahepatic metastasis. In contrast, only 2 CLC

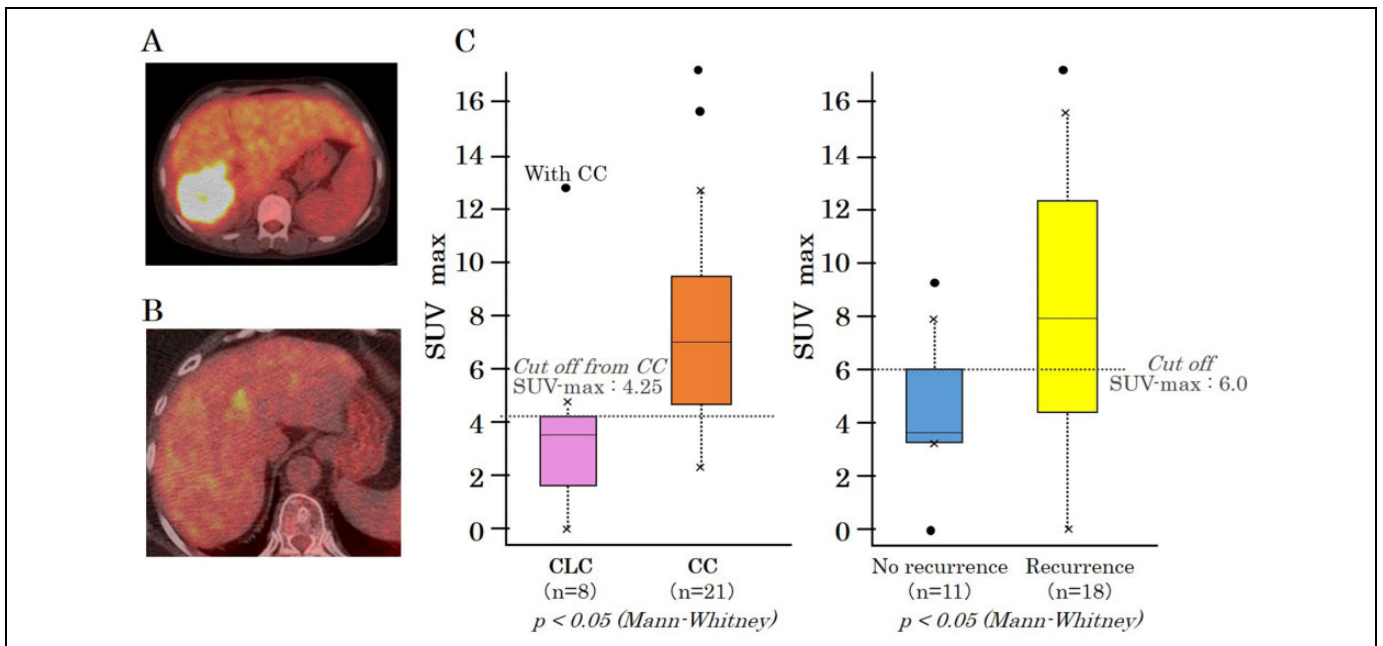


**Figure 7.** Primary tumor SUVmax on FDG-PET in patients with CLC or CC. Primary tumor SUVmax was significantly lower in patients with CLC than in those with CC. Patients without recurrence had significantly lower primary tumor SUVmax than those with recurrence, for both CLC and CC. FDG-PET may thus be useful for the differential diagnosis of CLC and CC and for predicting prognosis in patients with CLC or CC. A: FDG-PET (SUVmax: early 11.7, delayed 12.8) in complex CLC case with invasive CC component. B: FDG-PET (SUVmax: early 3.8, delayed 3.6) in pure CLC case. C: Comparison of primary tumor SUVmax between CLC and CC and between recurrence and no-recurrence in CLC and CC. Abbreviations: CC, cholangiocarcinoma; CLC, cholangiolocellular carcinoma; CT, computed tomography; FDG-PET, 18-fluoro-2-deoxyglucose positron-emission tomography; SUV, standardized uptake value.

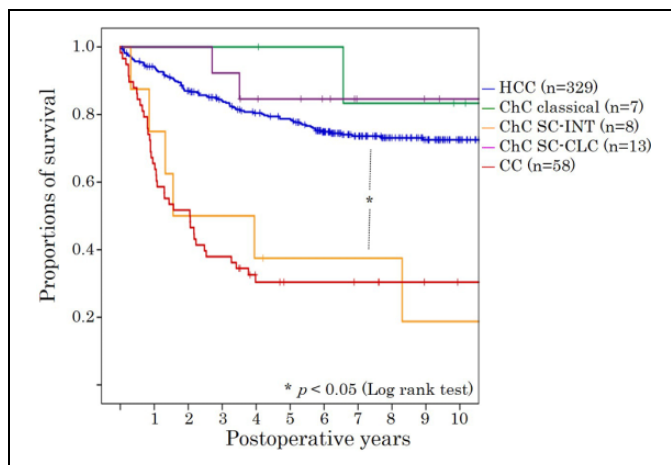


**Figure 8.** Overall survival curves for patients with primary liver cancer according to histological features. HCC, classical-type ChC, and CLC had significantly better prognoses than SC-INT and CC. Abbreviations: CC, cholangiocarcinoma; ChC, combined hepatocellular and cholangiocarcinoma; ChC classical, classical type ChC; CLC, cholangiolocellular carcinoma; HCC, hepatocellular carcinoma; SC-INT, intermediate cell subtype of ChC with stem cell features.

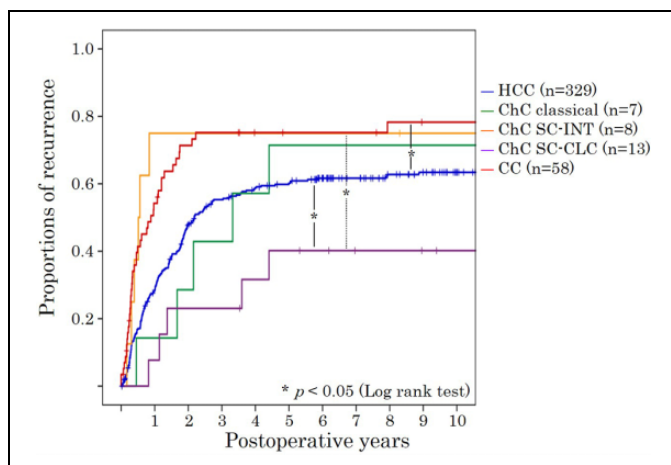


**Figure 9.** Progression-free survival in patients with primary liver cancer according to histological features. HCC and CLC had significantly lower recurrence rates than SC-INT and CC. CLC had significantly lower recurrence than HCC. CLC therefore had the best prognosis. Abbreviations: CC, cholangiocarcinoma; ChC, combined hepatocellular and cholangiocarcinoma; ChC classical, classical type ChC; CLC, cholangiolocellular carcinoma; HCC, hepatocellular carcinoma; SC-INT, intermediate cell subtype of ChC with stem cell features; SC typical, typical subtype of ChC with stem cell features.

patients had lymph node metastasis; however, the lymph node histology in both these cases was CC only, and both patients died of recurrence. This finding supports the idea that CLC should be regarded as a subtype of CC.

Mucin production is one of the features of cancer cells originating from the bile duct, but it is also observed at a constant frequency in ChC, reflecting the mixture of CC components.

Although early enhancement and early washout with corona-like staining on CT and angiography-assisted CT are

**Table 3.** Multivariate Analysis of Overall Survival Among Patients With HCC, ChC, or CC Who Underwent Hepatectomy, Including LDLT, According to Cox's Proportional Hazard Model That Included Significant Prognostic Indicators From Univariate Analysis.

Factor	Hazard Ratio (99% C.I.)	<i>p</i> value
Stage I–III	—	—
Stage IV	2.521 (1.576–4.033)	0.00000
HCC, Classic, CLC	—	—
SC-INT, CC	3.424 (2.080–5.631)	0.00000

Stage was evaluated according to the 6th edition (July 2015) of The General Rules for the Clinical and Pathological Study of Primary Liver Cancer established by the Liver Cancer Study Group of Japan (Kanehara Shuppan, Tokyo, Japan, 2015).

Abbreviations: Classic, classical type ChC; CLC, cholangiolocellular carcinoma (ChC SC subtype); CI, confidence interval; LDLT, living-related donor liver transplantation; SC-INT, intermediate cell subtype of ChC with stem cell features (ChC SC subtype).

considered specific to HCC, they were also frequently observed in SC-INT and classical ChC tumors, but were only detected in 1 case of CLC and in no cases of CC. In contrast, positive prolonged staining was characteristic of CLC and CC, whereas intratumoral Glisson's pedicle and hepatic vein penetration were specific to CLC and were not found in other tumor types, including CC. Intratumoral portal vein and hepatic vein penetration are difficult to recognize with regular enhanced multi-detector CT, and angiography-assisted CT may thus be useful for recognizing these features.

FDG-PET was useful for discriminating between CLC and CC, whereas HCC was characterized by almost no FDG accumulation.

Regarding the prognosis, HCC, classical ChC, and CLC were associated with significantly better overall survival rates than SC-INT and CC. The recurrence rate was lowest for CLC, but higher for HCC and classical ChC, which had higher frequencies of multicentric recurrence. CC had the worst prognosis, with both low overall survival and high recurrence. All recurrences of CC were metastatic, whereas multicentric recurrence was more common in HCC and classical ChC, suggesting that a good prognosis could be expected with additional appropriate treatment. Five patients with CLC had intrahepatic recurrence, including 3 with multicentric intrahepatic recurrence who underwent additional treatments with successful outcomes. The other 2 advanced cases showed progression to the hepatic hilum, lymph node metastasis, and metastatic recurrence of the CC component. The above observations suggest that CLC should be regarded as a subtype of CC.

## Discussion

We focused our attention on the diagnostic imaging, clinical and histopathological factors, and surgical treatment of CLC among ChC subtypes according to the WHO classification<sup>1</sup> (Theise ND, Nakashima O, Park YN, 2010). However, we hypothesized that CLC should be classified as a subtype of peripheral CC with similarities to bile ductules or canal of

Hering<sup>2</sup> because of its progression to the hepatic hilum with differentiation into CC and resulting lymph node metastasis. Although the frequency of liver cirrhosis was low among patients with CLC, chronic hepatitis C was relatively frequent; therefore, CLC cases exhibited multicentric recurrence of the HCC component, but not of the CLC component. These observations suggest that CLC clearly differentiates into cholangiocytes and should thus be regarded as a subtype of CC.

We determined the relative area occupied by each histological component on the largest split surface of 32 tumors diagnosed as ChC or CC mixed with other histological components. Although all classical ChC cases were mixed with CC, only one was mixed with CLC. Tumors with both an AFP- and HepPar1-positive HCC component and CC component of  $\geq 10\%$  were diagnosed as classical ChC; adding the 2 cases diagnosed as CC because they included  $< 10\%$  HCC component resulted in a total of 9 classical ChC cases according to these expanded criteria. Four of these 9 classical cases died of cancer, and as reported previously,<sup>15,16</sup> tumors meeting the classical criteria have a poorer prognosis than HCC. Among these 9 patients, the 4 who died of cancer had relatively high proportions of CC component, and metastasis of the CC component was presumed to be the main cause of death. Only 2 of the 9 classical ChC cases had clear CLC components. Because of the mixture of histological components, both HCC and CLC would be considered to have the same origin. However, as seen in the patient with glycogen storage disease type 1a, when HCC, CLC, and CC were all present, the CLC component was always present between the HCC and CC components, indicating that CLC should be regarded as a transition to CC. In contrast, SC-INT was not present with typical HCC component, whereas it was present with CLC or CC component.

As noted previously,<sup>7</sup> SC-INT may coexist with predominant CLC, and only 45.2% of cases showed SC-INT predominance. Notably, a higher proportion of SC-INT was significantly associated with larger tumor size and higher histological grade of the co-existing HCC. The proliferative activity of SC-INT was also significantly higher than that of CLC. In contrast, a higher proportion of CLC was significantly associated with smaller size and lower histological grade of HCC. These findings highlight the different properties of the SC-INT and the CLC subtypes, with SC-INT possibly representing a high-grade ChC with more aggressive behavior and CLC a low-grade ChC with an indolent nature. Furthermore, the different histological grading of HCC may indicate the different pathways of SC-INT and CLC in the stepwise progression of ChC. SC-INT may develop in the late stage of advanced HCC, which usually has a high histological grade. However, the molecular mechanisms in the stepwise progression of ChC remain unclear, and further studies are needed to elucidate this hypothesis. The findings of the current study and those of the previous study by Sasaki et al.<sup>7</sup> suggest that SC-INT could be considered distinct from HCC and classical ChC. Similar to CLC, SC-INT would be presumed to be a histological type intermittent between HCC and CC, but its poor prognosis and

high progression suggest that it should be clearly distinguished from classical ChC and CLC.

Sasaki et al. investigated the molecular biological characteristics, including genetic mutations, of each ChC subtype.<sup>8</sup> They found that AT-rich interactive domain-containing protein 1A (ARID1A), which is involved in remodeling of chromatin mutations, was significantly associated with CLC-subtype predominance ( $p < 0.05$ ), whereas telomerase reverse transcriptase (TERT) promoter mutations correlated with classical and SC-INT subtype-predominant histology, higher clinical stage, and a higher N-factor ( $p < 0.05$ ). Mutational analysis revealed that ChC had diverse mutations, and that mutations in the TERT promoter and ARID1A may reflect the etiology, histological subtype, histogenesis, and tumor aggressiveness. These results suggest the potential efficacy of a molecular-based subclassification of ChC and also support the notion of CLC as distinct from other ChC subtypes.

EMA, which is glycosylated-MUC1, is an immunohistochemical marker of CLC and CC. Sasaki et al. reported that MUC1 mRNA was extensively expressed in the intrahepatic bile duct by in situ hybridization and was consistent with EMA stainability, whereas MUC1/DF3 (CA15-3) was unstained in non-neoplastic bile ducts but stained in CLC and CC.<sup>17-19</sup> These results support the classification of CLC as a subtype of CC rather than a subtype of ChC.

Moeini et al.<sup>20</sup> also provided molecular biological evidence that affirms our theory that CLC should be considered a subtype of CC rather than a subtype of ChC. Their study revealed that CLC stands alone as a distinct biliary-derived entity associated with chromosomal stability and active TGF- $\beta$  signaling without the traits of HCC, unlike other ChC subtypes, such as classical type and SC-INT subtype. Molecular analysis of ChC showed that CLC is distinct and biliary in origin.

The specific imaging findings of CLC further suggest that it should be regarded as a subtype of CC rather than a subtype of ChC. The detailed imaging findings of pure CLC have been described previously.<sup>9</sup> Briefly, HCC, classical ChC, and SC-INT subtype commonly demonstrate washout and corona enhancement in the PP and/or EP on dynamic CT, angiography-assisted CT, and magnetic resonance imaging, findings that are not seen in pure CLC. Differentiating CLC from scirrhous-type HCC may be difficult in the case of early enhancement in the AP phase; however, radiological images and gross features of scirrhous HCC in early-phase CTHA show ring-like enhancement at the periphery of the nodule, and delayed-phase images reveal washout of contrast medium at the periphery but gradual enhancement in the center of the tumor.<sup>21</sup>

CLC presents with similar findings to HCC, such as hyper-vascular tumor in the AP, peritumoral enhancement, and either ring-like or wedge-shaped enhancement in the AP. We attribute these findings to the presence of cancer cell nests interspersed with abundant fibrous stroma and possible early drainage of contrast medium from the intratumoral blood sinusoids through the abundant communications between surrounding hepatic sinusoids and intermingled portal venules resulting

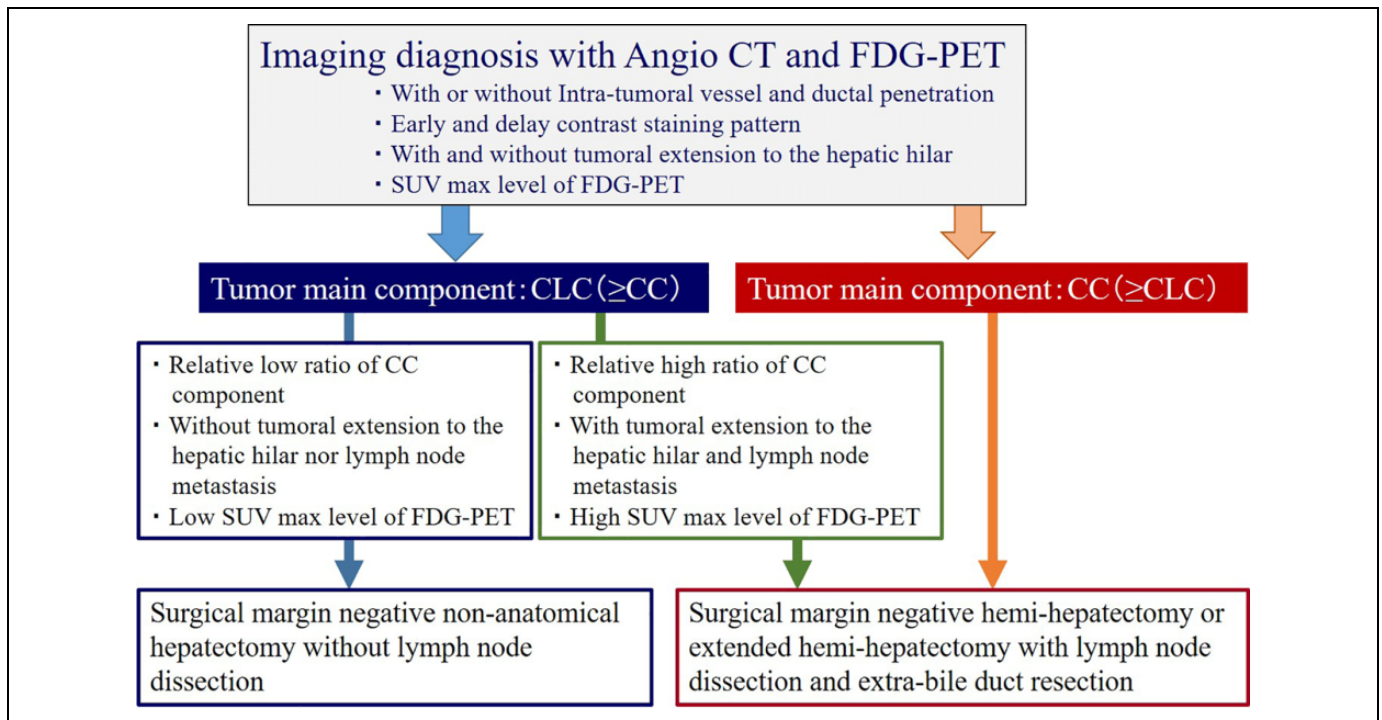


**Figure 10.** Surgical treatment algorithm for ChC and CC. Anatomical wide hepatectomy with extrahepatic bile duct resection and lymph node dissection is necessary for cure of CC and for CLC with extension to the hepatic hilum. CLC without progression can be cured even with non-anatomical hepatectomy if the surgical margin is secured, as for HCC, classical type ChC, and SC-INT.

Abbreviations: angio-CT, angiography-assisted CT; CC, cholangiocarcinoma; ChC, combined hepatocellular and cholangiocarcinoma; ChC classical, classical type ChC; CLC, cholangiolocellular carcinoma; HCC, hepatocellular carcinoma; SC-INT, intermediate cell subtype of ChC with stem cell features; SC typical, typical subtype of ChC with stem cell features; CT, computed tomography; FDG-PET, 18-fluoro-2-deoxyglucose positron-emission tomography; SUV, standardized uptake value.

from the replacing growth feature of pure CLC. These imaging features differ from those of other ChC subtypes and CC.<sup>9</sup> However, it is easy to distinguish CLC from other histological types because of the presence of intratumoral portal vein and hepatic vein penetration and lack of peripheral bile duct dilatation, even with large tumors. These specific findings of CLC are characterized by replacement growth and abundant stroma.

CTAP is useful for confirming portal vein perfusion defects and intratumoral portal vein and hepatic vein penetration because it reveals blood draining from the tumor into the intratumoral portal venules. CTHA images under angiography-assisted CT are also useful for confirming peritumoral enhancement observed in pure CLC and for distinguishing between hypervascular HCC and other ChCs.

A previous case report suggested that FDG-PET may be useful for distinguishing between CLC and CC.<sup>22</sup> In the current study, we confirmed the value of FDG-PET for distinguishing CC and also revealed its use as an indicator of recurrence. However, FDG-PET was not performed in patients with HCC or other ChC, and it was therefore not possible to determine its usefulness for differentiating between CLC and HCC or other ChCs.

LDLT was performed in patients with HCC and also in 3 patients with ChC (Table S2). One LDLT patient with ChC

who did not meet the Milan criteria developed recurrence; the 2 other patients, who met the Milan criteria, survived without relapse. Although ChC is generally recognized as a contraindication for liver transplantation,<sup>14</sup> these cases suggest that liver transplantation is not necessarily contraindicated in patients with ChC who meet the Milan criteria. However, worldwide, large-scale, multicenter trials are needed to confirm this.

The suggested treatment strategy for CLC and CC is shown in Figure 10. If preoperative imaging reveals CLC without progression to the hepatic hilum, without extrahepatic lymph node metastasis, and with an SUVmax on FDG-PET below the cut-off value for CC, curability is expected to be unimpaired, even with non-anatomical resection, if surgical margins are clear. This conclusion is supported by the fact that only 2 of 13 CLC cases had metastatic recurrence, progression to the hepatic hilum, and lymph node metastasis, whereas the other 11 cases with intrahepatic tumor localization had no metastatic recurrence, except for multicentric recurrence. Therefore, anatomical wide hepatectomy should not be necessary if the surgical margins can be secured. As reported by Ariizumi et al.,<sup>23</sup> CLC has a better prognosis than CC, without the need for anatomical wide hepatectomy.

In contrast, CLC with progression to the hepatic hilum, lymph node metastasis, or higher SUVmax on FDG-PET

requires wide hepatectomy as for CC. In these cases, hemihepatectomy with systematic lymph node dissection, extrahepatic bile duct resection, and biliary reconstruction are needed to effect a cure. Detailed preoperative histological imaging evaluation will inform the selection of the optimal surgical procedure and thus avoid under- or over-operation, with consequent patient benefits.

Neoadjuvant and adjuvant chemotherapy have not been established for the treatment of ChC, including CLC. We recently administered adjuvant gemcitabine (GEM) adjuvant chemotherapy in patients with CLC and CC with lymph node metastasis, and switched to S-1 therapy after relapse. Intravenous cisplatin (CDDP) and 5-fluorouracil were administered as adjuvant chemotherapy before GEM therapy. The prognosis of patients with recurrent CC was significantly improved after the introduction of GEM and S-1. In addition, GEM and S-1 had a favorable effect on patient prognosis, even among patients with stage IVA or IVB CLC or CC (Figures S3, S4). In addition, GEM and S-1 therapy significantly extended disease-free survival and survival after recurrence, suggesting that they were effective as both an adjuvant and as a treatment after recurrence (data not shown). Although we did not administer GEM and S-1 combination therapy and were therefore unable to evaluate the synergistic effect, clinical trials of GEM and S-1 combination therapy and GEM, S-1, and CDDP triple therapy are currently being conducted, and an evaluation of their effectiveness is awaited. Furthermore, the current sample size was small, and large prospective studies are needed to determine the efficacy of GEM and S-1.

In this study, the number of patients with ChC, including CLC, was small, and therefore the scientific evidence for statistical analysis was not sufficient. To raise the level of statistical evidence, future large-scale multicentric studies are needed.

## Conclusion

The 2010 WHO classification<sup>1</sup> classifies CLC as a ChC SC subtype. However, CLC component was mixed with CC component, and CC components were detected in CLC that progressed to the hepatic hilum, in perineural invasion and in lymph node metastases. The diagnostic imaging can clearly distinguish CLC from other ChC subtypes by the presence of intratumoral Glisson's pedicle, hepatic vein penetration, and tumor-staining pattern on angiography-assisted CT. CLC was associated with a significantly lower SUV-max than that of CC on FDG-PET. CLC has a good prognosis unless it progresses to the hepatic perihilar area. So that, from the viewpoint of surgeon, CLC should be classified as a good-prognosis subtype of intra-hepatic biliary tract carcinoma.

## Acknowledgments

We thank Rebecca Tollefson, DVM, of Edanz Group (<https://en-author-services.edanzgroup.com/>) for editing a draft of this manuscript.

## Declaration of Conflicting Interests

All authors report no proprietary or commercial interest in any product mentioned or concept discussed in this article. This research received no specific grant from any funding agency in the public, commercial, or not-for-profit sectors.


## Declaration of Conflicting Interests

The author(s) declared no potential conflicts of interest with respect to the research, authorship, and/or publication of this article.

## Funding

The author(s) received no financial support for the research, authorship, and/or publication of this article.

## ORCID iD

Hiroyuki Takamura  <https://orcid.org/0000-0002-8824-6763>

## Supplemental Material

Supplemental material for this article is available online.

## References

1. Theise ND, Nakashima O, Park YN, et al. *WHO Histological Classification of Tumours of the Liver and Intrahepatic Bile Ducts. WHO Classification of Tumours of the Digestive System*. IARC Press; 2010:225-227. <http://w2.iarc.fr/en/publications/pdfs-online/pat-gen/bb2/bb2-chap8.pdf>
2. Kozaka K, Sasaki M, Fujii T, et al. A subgroup of intrahepatic cholangiocarcinoma with an infiltrating replacement growth pattern and a resemblance to reactive proliferating bile ductules: "bile ductular carcinoma." *Histopathology*. 2007;51(3):390-400.
3. Sasaki M, Sato H, Kakuda Y, Sato Y, Choi JH, Nakanuma Y. Clinicopathological significance of "subtypes with stem-cell feature" in combined hepatocellular-cholangiocarcinoma. *Liver Cancer*. 2010;35(3):1024-1035.
4. Komuta M, Spee B, Borghet S, et al. Clinicopathological study on cholangiolocellular carcinoma suggesting hepatic progenitor cell origin. *Hepatology*. 2008;47(5):1544-1556.
5. Akiba J, Nakashima O, Hattori S. Clinicopathologic analysis of combined hepatocellular-cholangiocarcinoma according to the latest WHO classification. *Am J Surg Pathol*. 2013;37(4):496-505.
6. Sasaki M, Matsubara T, Kakuda Y, Sato Y, Nakanuma Y. Immunostaining for polycomb group protein EZH2 and senescent marker p16INK4a may be useful to differentiate cholangiolocellular carcinoma from ductular reaction and bile duct adenoma. *Am J Surg Pathol*. 2014;38(3):364-369.
7. Sasaki M, Sato H, Kakuda Y, Sato Y, Choi JH, Nakanuma Y. Clinicopathological significance of "subtypes with stem-cell feature" in combined hepatocellular-cholangiocarcinoma. *Liver Int*. 2015;35(3):1024-1035.
8. Sasaki M, Sato Y, Nakanuma Y. Mutational landscape of combined hepatocellular carcinoma and cholangiocarcinoma, and its clinicopathological significance. *Histopathology*. 2016;70(3):423-434.
9. Kozaka K, Matsui O, Kobayashi S, et al. Dynamic CT findings of cholangiolocellular carcinoma: correlation with angiography-



- assisted CT and histopathology. *Abdom Radiol.* 2017;42(3): 861-869.
10. Brunt E, Aishima S, Clavien PA, et al. cHCC-CCA: Consensus terminology for primary liver carcinomas with both hepatocytic and cholangiocytic differentiation. *Hepatology.* 2018;68(1): 113-126. doi:10.1002/hep.29789
  11. Steiner PE, Higginson J. Cholangiolocellular carcinoma of the liver. *Cancer.* 1959;12(4):753-759.
  12. Nakamura T, Ozawa T, Kawasaki T, Nakamura H, Sugimura H. Glucose-6-phosphatase gene mutations in 20 adult Japanese patients with glycogen storage disease type 1a with reference to hepatic tumors. *J Gastroenterol Hepatol.* 2001;16(12):1402-1408.
  13. Matsumoto T, Takai A, Eso Y, et al. Proliferating EpCAM-positive ductal cells in the inflamed liver give rise to hepatocellular carcinoma. *Cancer Res.* 2017;77(22):6131-6143.
  14. Chang CC, Chen YJ, Huang TH, et al. Living donor liver transplantation for combined hepatocellular carcinoma and cholangiocarcinoma: experience of a single center. *Ann Transplant.* 2017; 22:115-120.
  15. Shin DJ, Hong HS. Post-resection prognosis of combined hepatocellular carcinoma-cholangiocarcinoma according to the 2010 WHO classification. *World J Surg.* 2016;41(5):1347-1357.
  16. Shibahara J, Hayashi A, Misumi K, et al. Clinicopathologic characteristics of hepatocellular carcinoma with reactive ductule-like components, a subset of liver cancer currently classified as combined hepatocellular-cholangiocarcinoma with stem-cell features, typical subtype. *Am J Surg Pathol.* 2016;40(5):608-616.
  17. Sasaki M, Nakanuma Y, Kim YS. Characterization of apomucin expression in intrahepatic cholangiocarcinomas and their precursor lesions: an immunohistochemical study. *Hepatology.* 1996; 24(5):1074-1078.
  18. Sasaki M, Nakanuma Y, Ho SB, Kim YS. Cholangiocarcinomas arising in cirrhosis and combined hepatocellular-cholangiocellular carcinomas share apomucin profiles. *Am J Clin Pathol.* 1998;109(3):302-308.
  19. Sasaki M, Ikeda H, Nakanuma Y. Expression profiles of MUC mucins and trefoil factor family (TFF) peptides in the intrahepatic biliary system: physiological distribution and pathological significance. *Prog Histochem Cytochem.* 2007;42(2): 61-110.
  20. Moeini A, Sia D, Zhang Z, et al. Mixed hepatocellular cholangiocarcinoma tumors: cholangiolocellular carcinoma is a distinct molecular entity. *J Hepatol.* 2017;66(5):952-961.
  21. Fujii T, Zen Y, Harada K, et al. Participation of liver cancer stem/progenitor cells in tumorigenesis of scirrhous hepatocellular carcinoma-human and cell culture study. *Hum Pathol.* 2008; 39(8):1185-1196.
  22. Takahashi Y, Sato S, Ishitobi H, Nagaoka M, Kobayashi Y. Intrahepatic cholangiolocellular and cholangiocellular carcinoma - differences in the 18F-FDG PET/CT findings. *Intern Med.* 2017;56(22):3027-3031.
  23. Ariizumi S, Kotera Y, Katagiri S, et al. Long-term survival of patients with cholangiolocellular carcinoma after curative hepatectomy. *Ann Surg Oncol.* 2014;21(suppl 3):S451-458. doi:10.1245/s10434-014-3582-0.